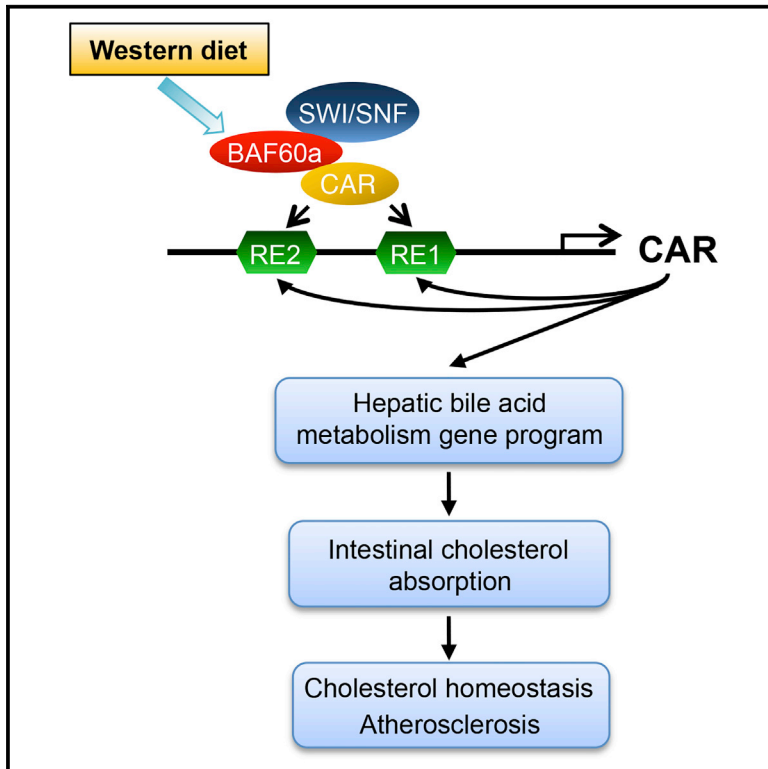# A Diet-Sensitive BAF60a-Mediated Pathway Links Hepatic Bile Acid Metabolism to Cholesterol Absorption and Atherosclerosis

Graphical Abstract

Authors

Zhuo-Xian Meng, Lin Wang, Lin Chang, ..., Yaqiang Li, Y. Eugene Chen, Jiandie D. Lin

Correspondence

zxmeng@umich.edu (Z.-X.M.),
jdlin@umich.edu (J.D.L.)

In Brief

Meng et al. find that Baf60a is a diet-sensitive subunit of the SWI/SNF complex and controls a hepatic gene program responsible for bile acid metabolism and intestinal cholesterol absorption through a Baf60a/CAR feedforward regulatory loop. Disruption of this pathway by liver-specific inactivation of Baf60a protects mice from diet-induced hypercholesterolemia and atherosclerosis.

Highlights

- Hepatic Baf60a is a diet-sensitive regulator of cholesterol homeostasis

- Hepatic Baf60a deficiency impairs bile acid metabolism and cholesterol absorption

- Baf60a/CAR form a feedforward regulatory loop to regulate bile acid metabolism genes

- Liver-specific Baf60a inactivation protects mice from diet-induced atherosclerosis

Accession Numbers
GSE73709

CellPress

Article

A Diet-Sensitive BAF60a-Mediated Pathway Links Hepatic Bile Acid Metabolism to Cholesterol Absorption and Atherosclerosis

Zhuo-Xian Meng,[1,*] Lin Wang,[1] Lin Chang,[2] Jingxia Sun,[1] Jiangyin Bao,[3] Yaqiang Li,[1] Y. Eugene Chen,[2] and Jiandie D. Lin[1,*]

[1]Life Sciences Institute and Department of Cell & Developmental Biology, University of Michigan, Ann Arbor, MI 48109, USA
[2]Center for Advanced Models for Translational Sciences and Therapeutics, Department of Internal Medicine, University of Michigan, Ann Arbor, MI 48109, USA
[3]Department of Chemistry, Michigan State University, East Lansing, MI 48824, USA
*Correspondence: zxmeng@umich.edu (Z.-X.M.), jdlin@umich.edu (J.D.L.)
http://dx.doi.org/10.1016/j.celrep.2015.10.033

SUMMARY

Dietary nutrients interact with gene networks to orchestrate adaptive responses during metabolic stress. Here, we identify Baf60a as a diet-sensitive subunit of the SWI/SNF chromatin-remodeling complexes in the mouse liver that links the consumption of fat- and cholesterol-rich diet to elevated plasma cholesterol levels. Baf60a expression was elevated in the liver following feeding with a western diet. Hepatocyte-specific inactivation of Baf60a reduced bile acid production and cholesterol absorption, and attenuated diet-induced hypercholesterolemia and atherosclerosis in mice. Baf60a stimulates expression of genes involved in bile acid synthesis, modification, and transport through a CAR/Baf60a feedforward regulatory loop. Baf60a is required for the recruitment of the SWI/SNF chromatin-remodeling complexes to facilitate an activating epigenetic switch on target genes. These studies elucidate a regulatory pathway that mediates the hyperlipidemic and atherogenic effects of western diet consumption.

INTRODUCTION

Elevated plasma low-density lipoprotein (LDL) cholesterol is a major risk factor for atherosclerosis and its associated cardiovascular mortality and morbidity (Glass and Witztum, 2001; Ross, 1993; Steinberg, 2002). The cholesterol pool in the body is tightly regulated by feedback mechanisms that impinge on endogenous cholesterol biosynthesis, catabolism, and excretion as bile acid (Chiang, 2009; Goldstein and Brown, 2015). Accumulation of intracellular sterol prevents the proteolytic activation of the sterol-response element binding protein (Srebp), transcriptional regulators of cholesterol biosynthesis, while stimulating the expression of genes involved in bile acid formation and excretion (Brown and Goldstein, 2009; Chiang, 2009). Phar-

macological targeting of these pathways has proved effective in lowering LDL cholesterol and reducing the risk of atherosclerosis (Expert Panel on Detection, Evaluation, and Treatment of High Blood Cholesterol in Adults, 2001; Grundy et al., 2004; Waters et al., 2009).

Nuclear hormone receptors have been implicated in sensing diverse metabolites in the cell, including lipids, oxysterols, bile acids, and xenobiotic compounds (Evans and Mangelsdorf, 2014). Hepatocytes sense the enterohepatic flux of cholesterol and bile acids in part through engaging liver X receptor (LXR) and farnesoid X receptor (FXR) (Calkin and Tontonoz, 2012; Matsubara et al., 2013). Oxysterols are oxygenated derivatives of cholesterol that serve as LXR ligands. A major target gene of LXR is Cyp7a1, which catalyzes the first step of the classic bile acid synthesis pathway (Lehmann et al., 1997; Peet et al., 1998). An alternative pathway initiated by sterol-27 hydroxylase (Cyp27a1) also contributes to cholesterol catabolism to bile acids (Schwarz et al., 2001). Bile acids are efficiently recycled through the enterohepatic circulation to facilitate intestinal absorption of dietary fats (Thomas et al., 2008). Accumulation of bile acids in hepatocytes results in FXR activation and induction of its target gene small heterodimer partner (Shp), which mediates the feedback inhibition of bile acid synthesis (Goodwin et al., 2000; Lu et al., 2000). In addition, constitutive androstane receptor (CAR) and pregnane X receptor (PXR), best known as xenobiotic sensors, regulate bile acid detoxification by stimulating the expression of hepatic genes responsible for the modification, conjugation, and transport of bile acids (Li and Chiang, 2013; Pascussi et al., 2008). Dietary intake of cholesterol is known to stimulate bile acid synthesis and increase bile acid pool and fecal excretion in rodents and humans; however, the nature of dietary regulation of bile acid homeostasis and intestinal lipid absorption remains elusive (Duane, 1994; Tiemann et al., 2004; Xu et al., 1999).

Nuclear receptors activate or repress gene transcription through recruiting various chromatin-remodeling complexes to alter the epigenetic landscape of target genomic loci (Chen and Roeder, 2011; Dasgupta et al., 2014; Mottis et al., 2013). Despite this, the significance of the nucleosome-remodeling
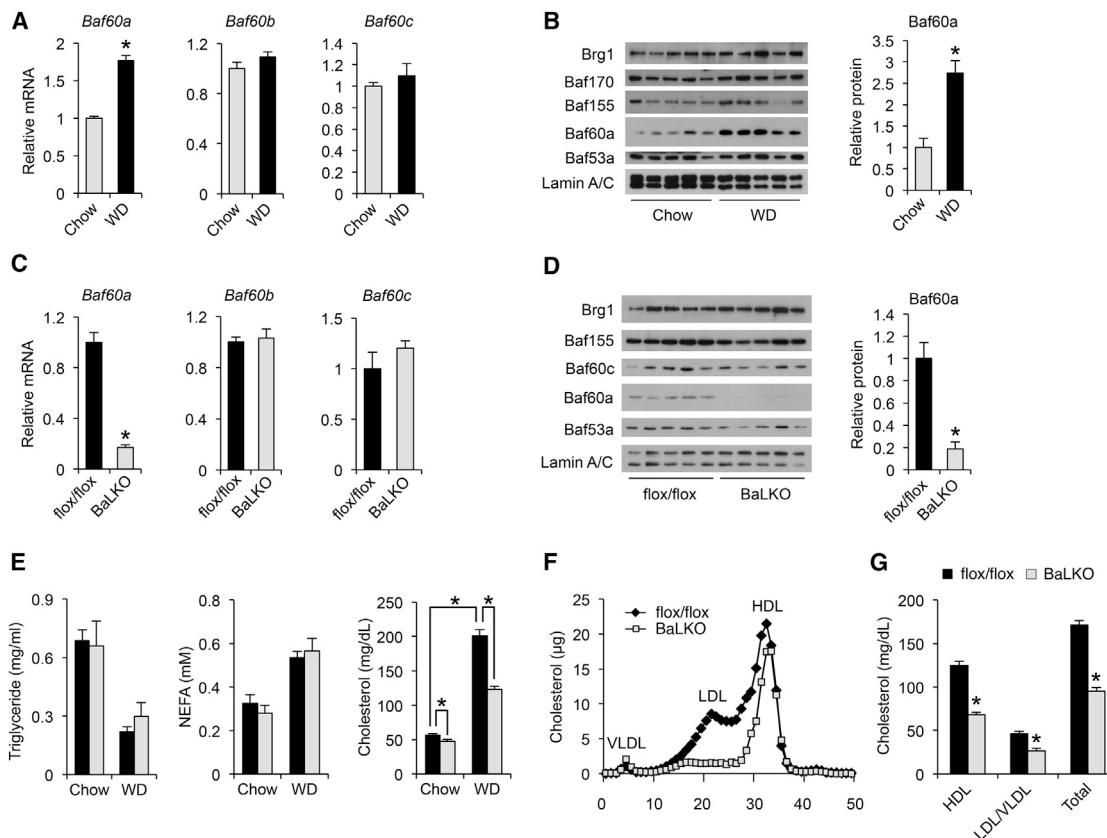
Figure 1. BaLKO Mice Are Resistant to Diet-Induced Hypercholesterolemia

(A) qPCR analysis of liver gene expression in mice fed standard chow or Western diet (WD) for 8 weeks (n = 5).

(B) Left, immunoblots of liver nuclear extracts; right, quantitation of Baf60a protein levels after normalization to Lamin A/C.

(C) qPCR analysis of gene expression in livers from flox/flox and BaLKO mice (n = 5).

(D) Left, immunoblots of liver nuclear extracts; right, quantitation of Baf60a protein levels after normalization to Lamin A/C.

(E–G) Plasma lipid levels (E), lipoprotein profile analysis (F), and concentrations of HDL, LDL/VLDL, and total cholesterol (G) in flox/flox and BaLKO mice following 12 weeks of WD feeding (n = 5). Values are mean ± SEM; *p < 0.05 by two-tailed Student's t test.

See also Figure S1.

complexes, such as the SWI/SNF complexes, in nuclear receptor signaling and metabolic physiology remains poorly understood. The SWI/SNF complexes are composed of one of two catalytic ATPase subunits (Brg1 or Brm) and additional subunits known as Brg/Brm-associated factors (Bafs) (Phelan et al., 1999; Sudarsanam and Winston, 2000; Wang et al., 1996; Wu et al., 2009). While Baf47, Baf170, and Baf155 form part of a core complex with Brg1/Brm, incorporation of other Baf subunits confers diversity and specificity of SWI/SNF complexes in transcriptional control. Recent studies have demonstrated that the Baf60 family members Baf60a and Baf60c recruit SWI/SNF complexes to regulate metabolic gene programs in the liver and skeletal muscle (Li et al., 2008; Meng et al., 2013, 2014). In this study, we identify Baf60a as a diet-sensitive factor in the liver that controls a hepatic gene program responsible for bile acid synthesis and intestinal cholesterol absorption through a Baf60a/CAR feed-forward regulatory loop. Disruption of this pathway by liver-specific inactivation of Baf60a protects mice from diet-induced hypercholesterolemia and atherosclerosis.

RESULTS

Hepatic Baf60a Is a Diet-Sensitive Regulator of Cholesterol Homeostasis

Chromatin-remodeling factors link nutrient signaling to metabolic gene programs through altering the epigenetic state of chromatin. The SWI/SNF complexes play an important role in differentiation, development, and tumorigenesis (Puri and Mercola, 2012; Wilson and Roberts, 2011); however, their role in diet-induced hyperlipidemia has not been explored. We analyzed the expression of core SWI/SNF subunits in the liver from mice fed standard chow or Western diet (WD); the latter has been commonly used to induce hypercholesterolemia. Immunoblotting analysis of liver nuclear extracts indicated that protein levels of core SWI/SNF subunits, including Brg1, Baf170, Baf155, and Baf53a, were similar between two groups (Figures 1A and 1B). In contrast, mRNA and protein levels of Baf60a were significantly elevated following WD feeding. The expression levels of Baf60b and Baf60c, two Baf60 family members closely related to Baf60a, remained largely insensitive to

diets. In addition, hepatic expression of Baf60a was similar between control and genetic obese mice (Figure S1A). Previous studies have demonstrated that Baf60a and Baf60c mediate the recruitments of the SWI/SNF complexes to specific target genes through their interaction with transcription factors and cofactors (Debril et al., 2004; Li et al., 2008; Meng et al., 2013). As such, Baf60a may serve as a diet-sensitive component of the SWI/SNF complexes in the liver that links dietary fat intake to lipid metabolism.

To dissect the role of Baf60a in mediating diet-gene interaction, we generated mice with conditional Baf60a deficiency in the liver. Mice containing floxed Baf60a alleles were crossed with Albumin-CRE (Alb-CRE) transgenic mice to generate control (flox/flox) and liver-specific Baf60a knockout mice (BaLKO, flox/flox:Alb-CRE) (Figure S1B). As expected, Baf60a mRNA and protein expression was markedly reduced in BaLKO mouse livers (Figures 1C and 1D). The expression levels of Baf60b, Baf60c, and other SWI/SNF subunits remained largely unaffected by Baf60a deficiency. Further, Baf60a expression in other metabolic tissues, including skeletal muscle, adipose tissues, and small intestine, was unaffected in BaLKO mice (Figures S1C and S1D). BaLKO mice were born at expected Mendelian ratio and appeared indistinguishable from control littermates. Plasma lipid concentrations were similar between two groups when fed standard chow, and, as expected, control mice exhibited elevated plasma cholesterol levels following 12 weeks of WD feeding (Figure 1E). In contrast, BaLKO mice were partially resistant to diet-induced hypercholesterolemia despite similar weight gain (Figures 1E and S1E); total plasma cholesterol concentration was approximately 40% lower in BaLKO mice than control. Plasma triglycerides (TAG), non-esterified fatty acids (NEFAs), and fasting blood glucose levels were similar between two groups following WD feeding (Figures 1E and S1F). Lipoprotein profile analysis and quantitative measurements of cholesterol in different lipoprotein fractions revealed that both LDL/very-low-density lipoprotein (VLDL) and high-density lipoprotein (HDL) cholesterol were lower in mice lacking Baf60a in the liver (Figures 1F and 1G). Together, these findings support a uniquely important role of Baf60a in mediating diet-induced elevation of plasma cholesterol levels.

Baf60a Deficiency in Hepatocytes Impairs Bile Acid Synthesis and Cholesterol Absorption

We next performed transcriptional profiling on the livers from WD-fed control and BaLKO mice to globally define hepatic target genes of Baf60a (GEO accession number GSE73709). Pathway analysis using the Database for Annotation, Visualization and Integrated Discovery (DAVID) revealed that a cluster of genes involved in primary bile acid biosynthesis was the most significantly downregulated gene set in response to Baf60a inactivation in hepatocytes (Figures 2A and 2B). Several nuclear hormone receptors, including FXR, LXR, CAR, and PXR, have been reported as important regulators of cholesterol and bile acid metabolism in the liver (Beaven and Tontonoz, 2006; Chiang, 2009; Evans and Mangelsdorf, 2014; Gao and Xie, 2012). While mRNA levels for PXR, LXR, and FXR remained largely unaltered by Baf60a deficiency, the expression of CAR

was markedly lower in BaLKO livers than control (Figure 2C). This decrease in CAR expression correlated with lower expression of genes involved in bile acid synthesis, including Cyp8b1, Cyp27a1, Cyp7b1, BAAT, and Hsd3b5, and those involved in xenobiotic responses and bile acid modification and transport, such as Cyp2b10, Cyp3a11, Sult5a1, Ugt1a1, Oatp2, Mrp3, and Mdr2 (Figure 2D). In contrast, the expression of Shp, a canonical target gene of FXR, and Cyp7a1, Abca1, Abcg5, and Abcg8, target genes of LXR, remained similar between two groups (Figure 2E). The expression of hepatic genes involved in cholesterol biosynthesis (Srebp1a, Srebp1c, Srebp2, Hmgcr, and Hmgcs1) appeared largely unaffected by Baf60a deficiency. Further, mRNA and protein levels of LDLR, which is responsible for the uptake of plasma LDL (Brown and Goldstein, 1986), and Pcsk9, an important modulator of LDLR protein levels (Horton et al., 2009), were comparable between control and BaLKO mice (Figures 2E–2G). Consistently, lipoprotein secretion analysis indicated that the rise of plasma cholesterol concentrations following tail-vein injection of tyloxapol (500 mg/kg) was unaffected by Baf60a deficiency (Figure S2A). As such, hepatic inactivation of Baf60a appears to exert modest effects on cholesterol synthesis, LDL uptake, and lipoprotein secretion. To rule out the possibility that Baf60a deficiency may impair liver function and cause liver injury, we measured plasma alanine transaminase (ALT) and aspartate aminotransferase (AST) levels, and the expression of marker genes involved in liver fibrosis and inflammation. Plasma concentrations of ALT and AST were significantly lower in BaLKO mice than control, whereas the mRNA expression of genes involved in liver fibrosis and inflammation remained similar between two groups (Figures S2B and S2C).

As bile acids play an important role in the digestion and absorption of dietary fats, impaired intestinal cholesterol absorption may contribute to resistance to diet-induced hypercholesterolemia in BaLKO mice. In support of this, total bile volume and biliary bile acid content were approximately 37% lower in BaLKO mice than control, whereas plasma and liver bile acid concentrations remained similar between two groups (Figures 3A and 3B). Measurements of bile acid pool indicated that liver/gallbladder and intestine bile acid pool sizes were both significantly lower in BaLKO mice, resulting in lower whole-body bile acid content (Figure 3C). However, the composition of different bile acid species in bile from gallbladder remained similar between two groups (Figure 3D). In parallel, liver cholesterol content is elevated in BaLKO mice compared to control (Figure 3E). Consistent with dietary cholesterol being an important source of the lipid, cholesterol-lowering effect of hepatic Baf60a deficiency was abolished following overnight starvation (Figure 3F). While food intake remained similar between two groups, cholesterol excretion in feces was significantly higher in BaLKO mice (Figure 3G), suggesting that hepatic Baf60a inactivation impaired intestinal cholesterol absorption. Direct measurements of cholesterol absorption by oral gavage of ^{3}H-labeled cholesterol indicated that the amounts of radiolabeled cholesterol in plasma and the liver were significantly lower in BaLKO mice than control (Figure 3H). Consequently, cholesterol-lowering effects of ezetimibe, an inhibitor of cholesterol absorption, failed to further reduce plasma cholesterol levels in
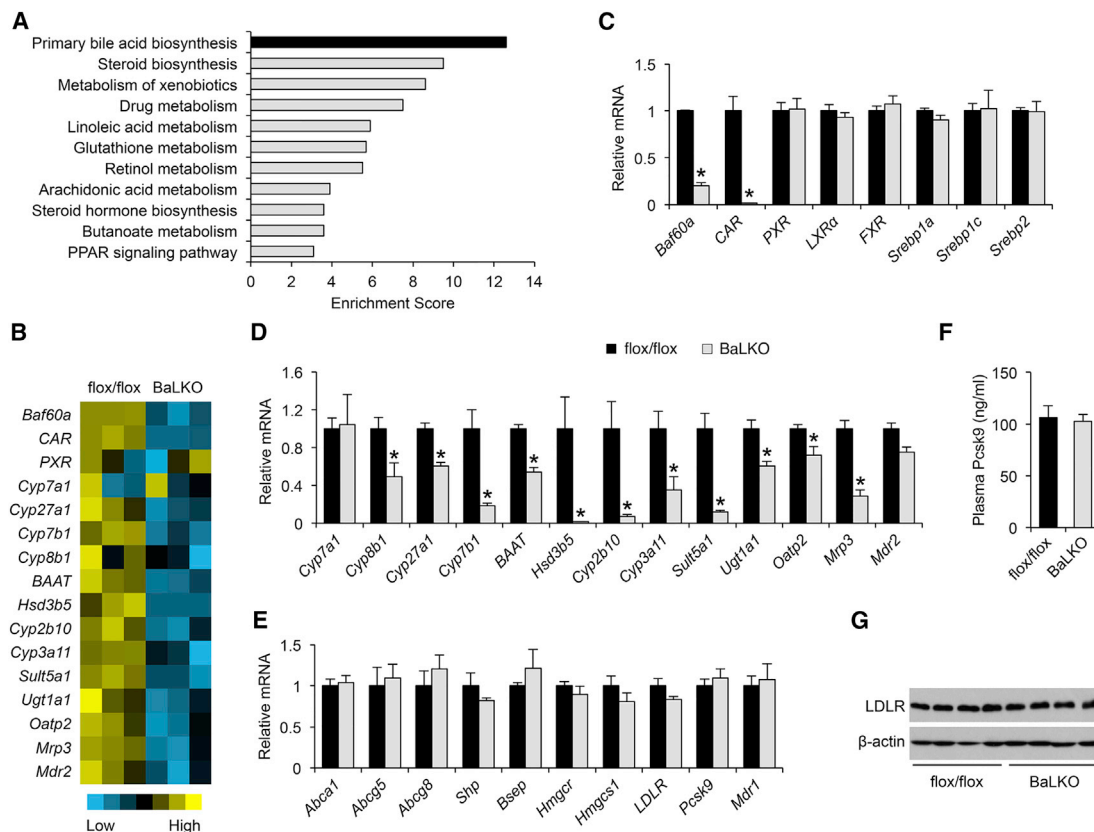
Figure 2. Baf60a Regulates CAR and Its Target Genes Involved in Bile Acid Metabolism
(A) DAVID pathway analysis of downregulated genes in BaLKO mouse livers identified by microarray.
(B) Heatmap representation of genes involved in bile acid metabolism.
(C–E) qPCR analysis of the mRNA expression of transcriptional factors (C), CAR target genes (D), and FXR, LXR and PXR target genes (E) involved in bile acid metabolism in livers from flox/flox and BaLKO mice fed with WD for 12 weeks (n = 5).
(F) Plasma concentrations of Pcsk9 (n = 4–5).
(G) Immunoblots of total liver lysates.
Data in (C)–(F) are mean ± SEM; *p < 0.05 by two-tailed Student's t test. See also Figure S2.

BaLKO mice (Figure 3I). These results illustrate that impaired cholesterol absorption secondary to reduced bile acid synthesis likely mediates resistance to diet-induced hypercholesterolemia in BaLKO mice.

Baf60a Cell-Autonomously Regulates the Bile Acid Metabolism Gene Program
The marked reduction of CAR expression in the BaLKO mouse livers suggests that its deficiency may be responsible for lower expression of genes involved in bile acid metabolism. We next examined whether Baf60a regulates CAR gene expression in a cell-autonomous manner. Gene expression analysis of primary hepatocytes isolated from flox/flox and BaLKO mice demonstrated that mRNA expression of *CAR* was approximately 74% lower in Baf60a-deficient hepatocytes (Figures 4A and 4B). In parallel, mRNA expression of several genes involved in the alternative pathway of bile acid synthesis, including *Cyp8b1*, *Cyp27a1*, and *Cyp7b1*, and bile acid modification and transport, including *BAAT*, *Hsd3b5*, *Cyp2b10*, *Cyp3a11*, *Sult5a1*, *Ugt1a1*, *Oatp2*, *Mrp3*, and *Mdr2*, was also

significantly lower in Baf60a-deficient hepatocytes. Treatments of hepatocytes with TCPOBOP, a synthetic CAR agonist, significantly induced mRNA expression of *Cyp2b10*, a canonical CAR target gene, and *CAR* itself. However, the induction of these two genes by TCPOBOP was nearly abolished in hepatocytes lacking Baf60a (Figure 4C), indicating that Baf60a is required for maintaining the expression and transcriptional activity of CAR in hepatocytes.

To determine whether Baf60a serves as an upstream regulator of CAR, we transduced primary hepatocytes with control GFP or Baf60a adenoviruses. Gene expression analysis indicated that adenoviral-mediated overexpression of Baf60a resulted in over 10-fold induction of endogenous CAR (Figures 4A and 4D). Importantly, Baf60a stimulated the expression of *Cyp8b1*, *Cyp27a1*, *Cyp7b1*, and a panel of genes involved in bile acid modification and transport. Baf60a-mediated induction of *CAR* and *Cyp2b10* was further augmented by TCPOBOP treatments, suggesting that Baf60a acts in concert with CAR to regulate the expression of CAR target genes (Figure 4E). To assess the effects of hepatic Baf60a activation on cholesterol
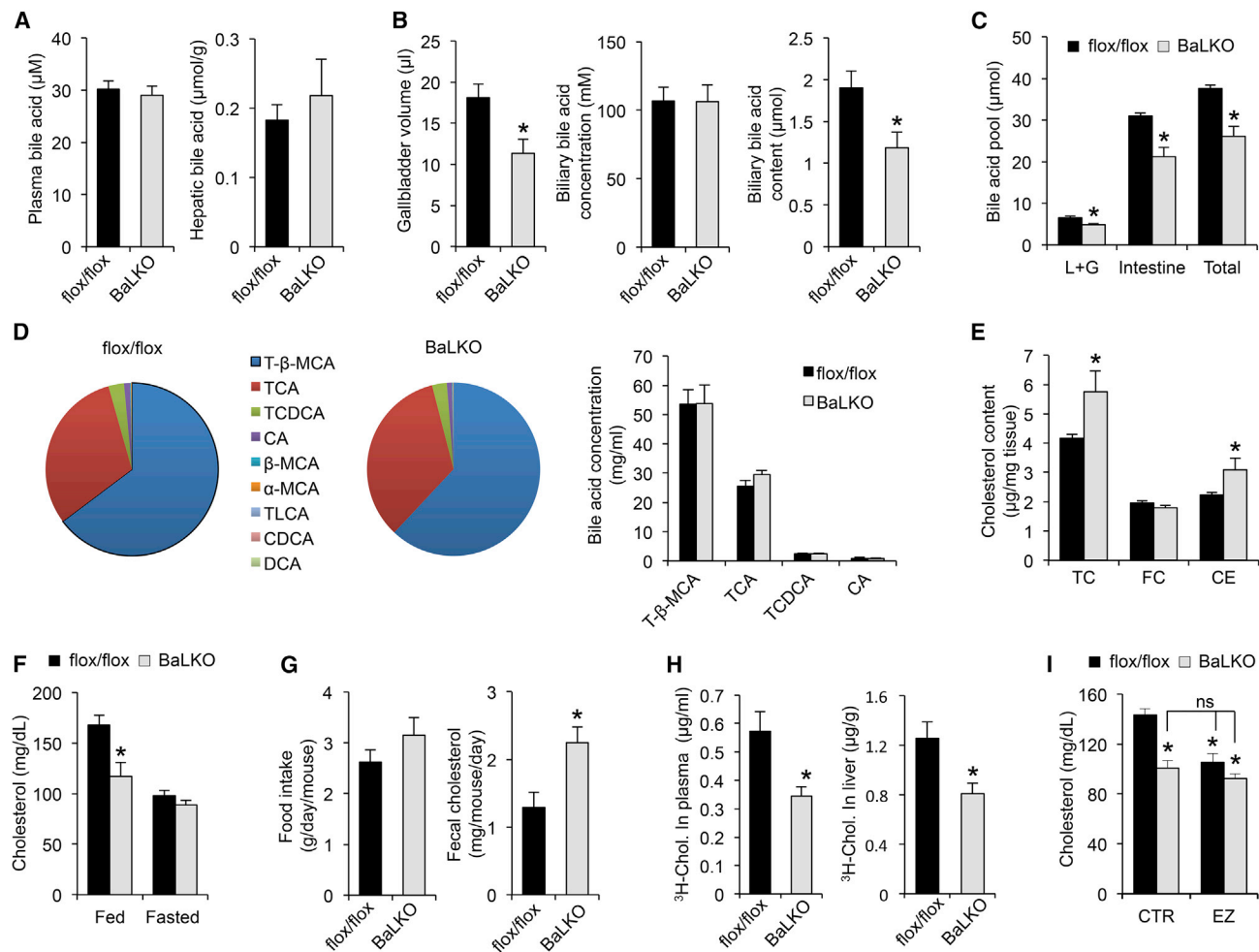
Figure 3. Hepatic Baf60a Regulates Bile Acid Metabolism and Cholesterol Absorption

flox/flox and BaLKO mice were fed with standard chow or WD for 12 weeks.

(A and B) Plasma and hepatic bile acid levels (A) and gallbladder volume, biliary bile acid concentrations, and biliary bile acid content (B) (n = 6–8).

(C) Bile acid pool size in liver plus gallbladder (L+G), intestine, and whole body (Total) (n = 5).

(D) Bile acid composition in the bile from gallbladder. Left, percentile composition of different bile acids in the bile from flox/flox and BaLKO mice; right, concentrations of four major bile acids in the bile. T-β-MCA, tauro-β-muricholic acid; TCA, taurocholic acid; TCDCA, taurochenodeoxycholic acid; CA, cholic acid; β-MCA, β-muricholic acid; α-MCA, α-muricholic acid; TLCA, taurolithocholic acid; CDCA, chenodeoxycholic acid; DCA, deoxycholic acid.

(E) Concentrations of total cholesterol (TC), free cholesterol (FC), and cholesterol ester (CE) in livers from control (dark bars) and BaLKO (gray bars) mice (n = 6–9).

(F) Plasma cholesterol levels in mice under fed and fasted conditions (n = 6).

(G) Food intake and fecal cholesterol content in WD-fed control and BaLKO mice (n = 4–5).

(H) Cholesterol uptake into plasma and liver following oral gavage of ^{3}H-cholesterol (^{3}H-chol.) for 2 hr.

(I) Plasma cholesterol concentrations in WD-fed control and BaLKO mice treated with vehicle alone (CTR) or ezetimibe (EZ) for 4 days (n = 6); *p < 0.05 versus flox/flox mice treated with vehicle alone; ns, not significant.

In all panels, values are mean ± SEM; *p < 0.05 by two-tailed Student's t test.

absorption in mice, we transduced WD-fed wild-type mice with recombinant adenoviruses expressing GFP or Baf60a via tail-vein injection. Compared to control, mice transduced with Baf60a adenovirus had significantly elevated total plasma cholesterol levels (Figure 4F). Gene expression analysis indicated that tail-vein transduction of Baf60a adenovirus significantly increased mRNA levels of *CAR* and its target genes in the liver (Figure 4G). The expression of *LXR*, *FXR*, *PXR*, *Srebp1a*, *Srebp1c*, *Srebp2*, and their target genes remained similar between two groups.

Baf60a and CAR Form a Feedforward Regulatory Loop through a SWI/SNF-Mediated Epigenetic Mechanism

The SWI/SNF chromatin-remodeling complexes are recruited to specific chromatin loci through physical interaction with transcription factors. The BAF60 subunit has been demonstrated to serve as a molecular link between the core complexes and DNA-binding factors (Li et al., 2008; Meng et al., 2013, 2014). To test whether Baf60a physically interacts with CAR, we performed protein-protein interaction assay using coimmunoprecipitation (coIP). Baf60a and CAR formed a physical complex
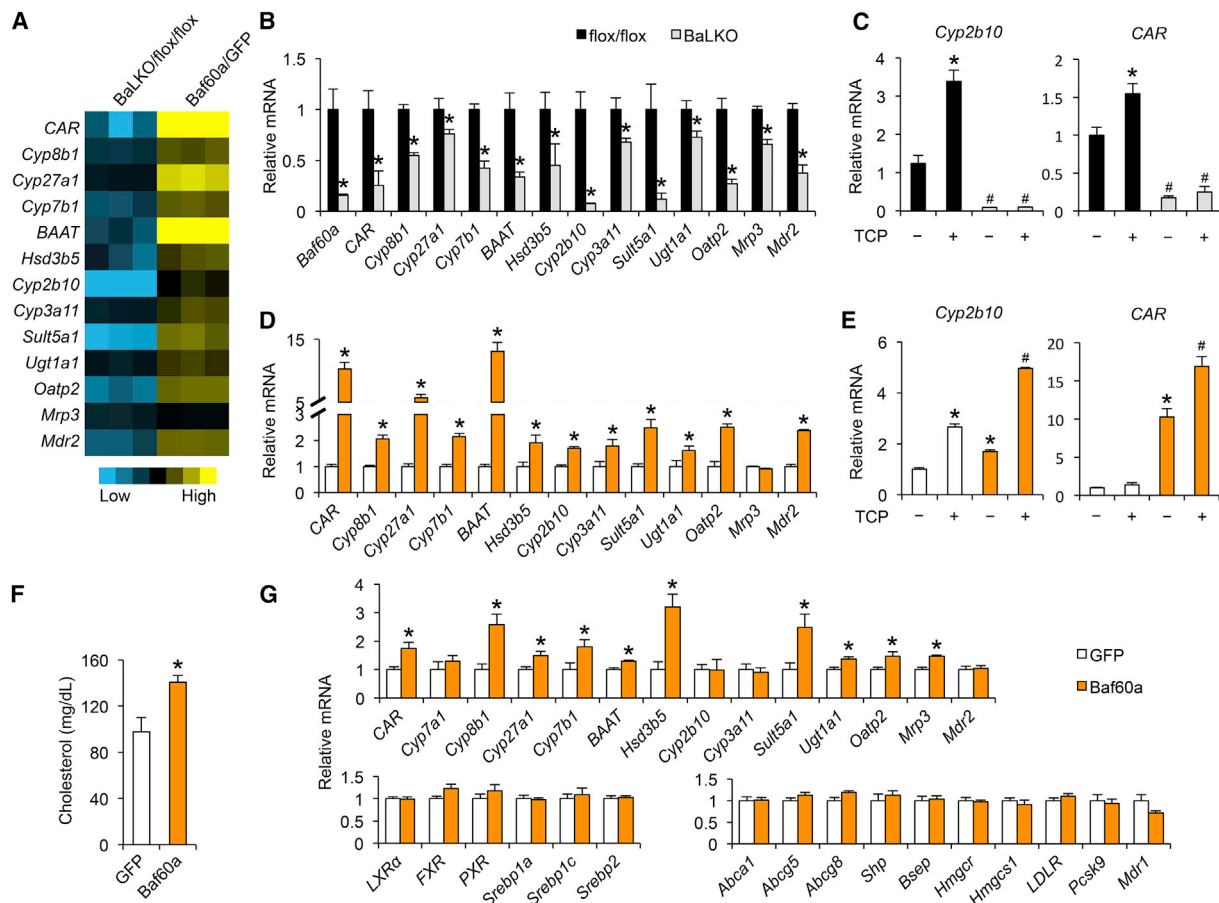
Figure 4. Baf60a Regulates the Bile Acid Metabolism Gene Program in a Cell-Autonomous Manner

(A) Heatmap representation of gene regulation in response to Baf60a deficiency (BaLKO/flox/flox) and Baf60a overexpression (Baf60a/GFP) in primary hepatocytes.

(B and C) qPCR analysis of gene expression in primary hepatocytes isolated from flox/flox and BaLKO mice in the presence or absence of TCPOBOP treatment (TCP, 1 μM) for 24 hr. In (C), *p < 0.05 versus vehicle treatment alone (the first bar); #p < 0.05 versus TCP treatment alone (the second bar).

(D and E) qPCR analysis of gene expression in primary hepatocytes transduced with GFP or Baf60a adenoviruses and treated with or without TCP 1 μM for 24 hr. *p < 0.05 versus GFP expression alone; #p < 0.05 versus TCP treatment or Baf60a expression alone.

(F) Plasma cholesterol levels in WD-fed WT mice transduced with adenoviruses expressing GFP or Baf60a.

(G) qPCR analysis of hepatic gene expression in WT mice transduced with adenoviruses expressing GFP or Baf60a.

Data in (B)–(E) represent mean ± SD and are representative of three independent experiments; data in (F) and (G) represent mean ± SEM (n = 6); #p < 0.05, and *p < 0.05 by two-tailed Student's t test.

when they were co-expressed in HEK293 cells following transient transfection (Figure 5A). The physical association between CAR and Baf60a was further confirmed in HepG2 hepatoma cells. We transduced HepG2 cells with adenoviruses expressing GFP or Flag/HA-tagged CAR (FH-CAR) and performed immunoprecipitation using anti-HA agarose beads. Immunoblotting analyses indicated that, in addition to endogenous Baf60a, other subunits of the SWI/SNF complexes, including Brg1, Baf170, Baf155, and Baf53a, were readily detectable in the CAR immunocomplexes (Figure 5B). These findings suggest that Baf60a mediates the recruitment of the SWI/SNF chromatin-remodeling complexes to the genomic targets occupied by CAR.

Genomatix motif analysis predicted two putative CAR Response Elements (CARRE) located approximately 2.0 (RE2) and 0.9 kb (RE1) upstream of the transcriptional start site of CAR gene. Chromatin immunoprecipitation (ChIP) assays demonstrated that epitope-tagged Baf60a and CAR were recruited to these two sites on the native CAR promoter (Figures 5C and 5D). As such, Baf60a and CAR appear to form a feedforward regulatory loop to drive the expression of CAR and its target genes. A prediction of this model is that Baf60a levels may dictate the recruitment of the SWI/SNF complexes, which, in turn, has an impact on the local epigenetic landscape. To test this, we performed ChIP assay in control and Baf60a-deficient primary hepatocytes. Baf60a deficiency significantly reduced the recruitment of SWI/SNF core subunit Brg1 to the chromatin near the CAR binding sites, leading to reduced levels of acetyl-histone H3 (Ace-H3) and trimethylation of H3 lysine 4 (H3K4m3), two epigenetic markers associated with
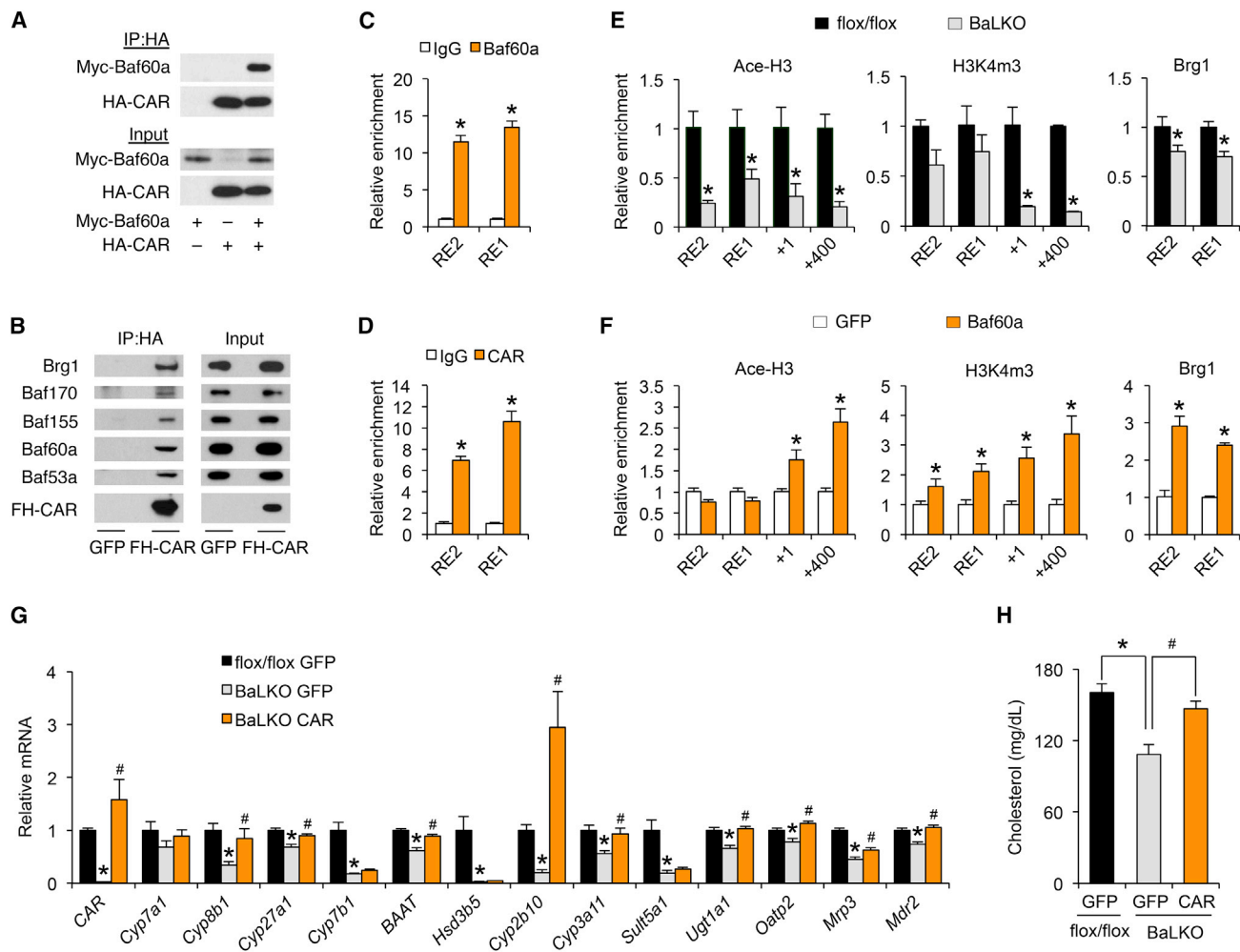
Figure 5. Baf60a and CAR Form a Feedforward Regulatory Loop

(A) Physical interaction between CAR and Baf60a in transiently transfected 293T cells. IP, immunoprecipitation; Myc-Baf60a, Myc-tagged Baf60a; HA-CAR, HA-tagged CAR.

(B) Immunoblots of immunoprecipitated proteins or total protein lysates from HepG2 cells transduced with adenoviruses expressing Flag/HA-tagged CAR (FH-CAR). Note that FH-CAR interacts with endogenous SWI/SNF subunits.

(C and D) Relative enrichment of Baf60a (C) and CAR (D) at the putative CAR binding site on the proximal CAR promoter. RE1, CAR response element 1; RE2, CAR response element 2.

(E) ChIP assay with chromatin lysates prepared from flox/flox and BaLKO mouse livers using indicated antibodies.

(F) ChIP assay with chromatin lysates prepared from primary hepatocytes transduced with GFP or Baf60a adenoviruses.

(G and H) WD-fed flox/flox and BaLKO mice were transduced with adenoviruses expressing GFP or CAR for 1 week. Shown are qPCR analysis of hepatic gene expression (G) and measurement of plasma cholesterol levels (H); *p < 0.05, BaLKO GFP versus flox/flox GFP; #p < 0.05, BaLKO CAR versus BaLKO GFP.

Data in (C)–(F) represent mean ± SD and are representative of three independent experiments; data in (G) and (H) represent mean ± SEM (n = 4–5); #p < 0.05, and *p < 0.05 by two-tailed Student's t test. See also Figure S3.

transcriptional activation (Figure 5E). Conversely, adenoviral-mediated expression Baf60a augmented the recruitment of Brg1 and increased Ace-H3 and H3K4m3 levels on the proximal CAR promoter (Figure 5F). There results demonstrate that Baf60a modulates the transcriptional activity of CAR through its recruitment of SWI/SNF-mediated chromatin remodeling.

The marked reduction of CAR expression in BaLKO mouse livers suggest that Baf60a deficiency may disrupt the feedforward regulatory loop and impair the transcription of CAR target genes. We next performed rescue studies to determine the sig-

nificance of CAR in mediating the effects of Baf60a deficiency on plasma cholesterol. Consistent with previous transgenic studies (Dong et al., 2009; Saini et al., 2004), tail-vein injection of CAR adenovirus significantly increased the expression of its target genes involved in bile acid metabolism in wild-type mice (Figures S3A–3C). Adenoviral-mediated rescue of CAR expression in BaLKO mice to slightly above its endogenous levels restored the expression of several CAR target genes, including *Cyp8b1*, *Cyp27a1*, *BAAT*, *Cyp2b10*, *Cyp3a11*, *Ugt1a1*, *Oatp2*, *Mrp3*, and *Mdr2* (Figure 5G), and more importantly, reversed plasma
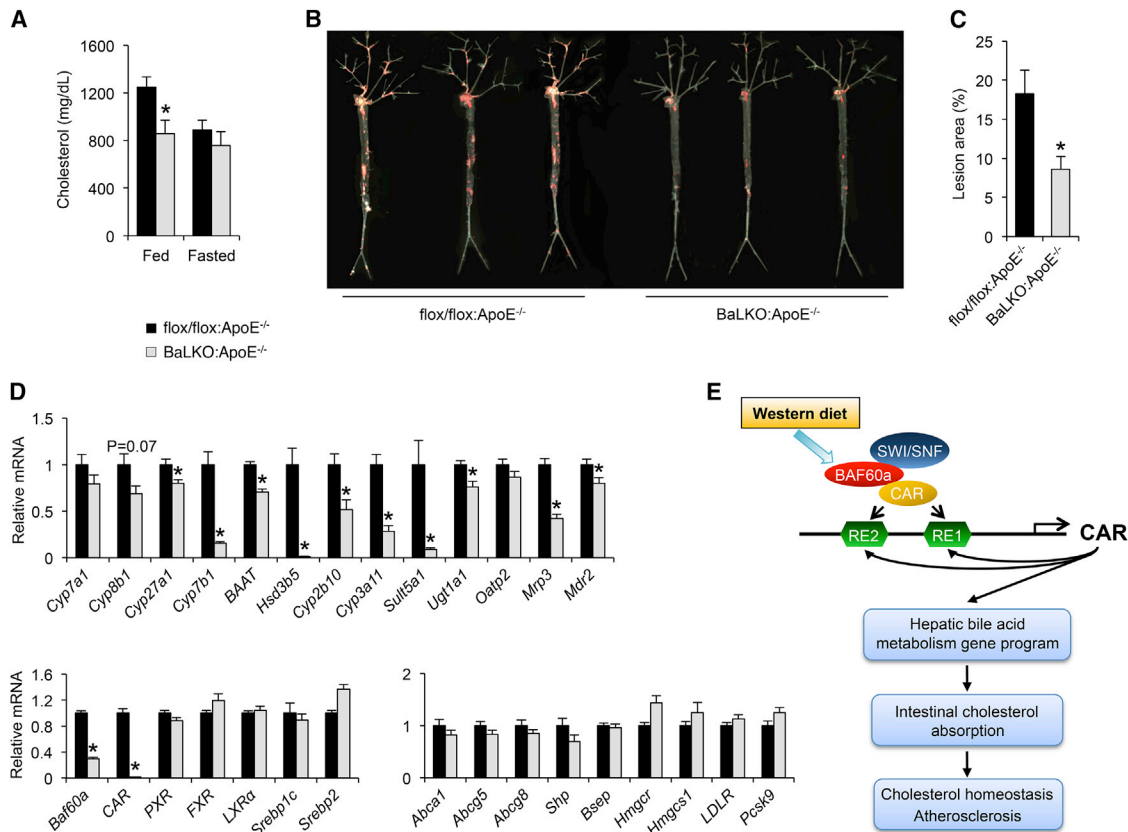
Figure 6. Hepatic Inactivation of Baf60a Protects Mice from Diet-Induced Atherosclerosis

(A) Fed and fasting plasma cholesterol levels in flox/flox:ApoE$^{-/-}$ and BaLKO:ApoE$^{-/-}$ mice fed with WD for 12 weeks (n = 6).

(B) Representative images of en face oil-red-O-stained aortic arches.

(C) Quantification of lesion area (n = 10–15).

(D) qPCR analysis of hepatic gene expression in flox/flox:ApoE$^{-/-}$ and BaLKO:ApoE$^{-/-}$ mouse livers (n = 6–9).

(E) Schematic model of the Baf60a/CAR feedforward regulatory loop in mediating diet-induced hypercholesterolemia and atherosclerosis.

Data shown in (A), (C), and (D) represent mean ± SEM; *p < 0.05 by two-tailed Student's t test.

cholesterol levels in BaLKO mice (Figure 5H). Although the expression *PXR* was not significantly altered in livers from BaLKO mice, our coIP experiments indicated that Baf60a could also physically interact with PXR (Figure S3D). As such, PXR may mediate the transcriptional effects of Baf60a on a subset of target genes involved in bile acid metabolism and xenobiotic detoxification. In support of this possibility, adenoviral expression of CAR failed to restore the expression of *Cyp7b1*, *Hsd3b5*, and *Sult5a1* in BaLKO mouse livers. We conclude from these studies that Baf60a activates a CAR-dependent program of gene expression in the liver to facilitate bile acid production and intestinal lipid absorption.

Liver-Specific Inactivation of Baf60a Protects Mice from Diet-Induced Atherosclerosis

Elevated LDL cholesterol is a major risk factor for atherosclerosis. ApoE plays an important role in the regulation of plasma cholesterol through its interaction with LDLR to facilitate the uptake of cholesterol-rich lipoproteins (Mahley, 1988). ApoE-null (ApoE$^{-/-}$) mice have markedly elevated plasma cholesterol levels and are a commonly used model of atherosclerosis (Ishibashi et al., 1994;

Piedrahita et al., 1992). To determine the significance of Baf60a in cholesterol homeostasis and atherosclerosis, we generated cohorts of flox/flox:ApoE$^{-/-}$ and BaLKO:ApoE$^{-/-}$ mice and subjected them to WD feeding. Plasma lipid measurements indicated that hepatocyte-specific inactivation of Baf60a lowered total plasma cholesterol levels by approximately 30% in ApoE$^{-/-}$ background (Figure 6A). The cholesterol-lowering effect was only observed in BaLKO:ApoE$^{-/-}$ mice under fed conditions. To elucidate the significance of hepatic Baf60a in atherosclerosis, we performed oil red O staining on the dissected arterial trees from flox/flox:ApoE$^{-/-}$ and BaLKO:ApoE$^{-/-}$ mice following 12 weeks of WD feeding. Remarkably, hepatocyte-specific inactivation of Baf60a significantly ameliorated atherosclerotic lesion formation (Figure 6B). Compared to control, lesion area was approximately 53% smaller in BaLKO mice (Figure 6C). Gene expression analysis indicated that the expression of CAR and its target genes involved in bile acid metabolism was significantly lower in BaLKO:ApoE$^{-/-}$ mouse livers (Figure 6D). Together, these results illustrate a diet-sensitive epigenetic pathway in the liver that plays a critical role in lipid absorption, cholesterol homeostasis, and atherosclerosis.

DISCUSSION

The interaction between dietary nutrients and the gene networks is pivotal for metabolic homeostasis and contributes to the pathogenesis of complex diseases. Chronic consumption of fat- and cholesterol-rich diet is known to elevate plasma cholesterol levels and increase the risk for cardiovascular diseases (Glass and Witztum, 2001; Ross, 1993; Steinberg, 2002). In this study, we identified Baf60a as a diet-sensitive subunit of the SWI/SNF chromatin-remodeling complexes in the liver that serves a critical role in elevating plasma cholesterol levels following WD feeding. Hepatocyte-specific inactivation of Baf60a partially protects mice from WD-induced elevation of plasma cholesterol levels and atherosclerosis. At the mechanistic level, hepatic Baf60a is required for maintaining bile acid homeostasis and intestinal cholesterol absorption through a CAR/Baf60a feedforward regulatory loop in the liver (Figure 6E).

Several lines of evidence support a crucial role of Baf60a in bile acid production and intestinal cholesterol absorption. Transcriptional profiling and pathway analysis indicated that the genes involved in primary bile acid biosynthesis ranked at the top among those downregulated by Baf60a deficiency. Interestingly, the expression of Cyp7a1, a target gene of LXR in the classic bile acid synthesis pathway, remained largely unchanged. In contrast, mRNA levels for the genes responsible for the alternative pathway of bile acid biosynthesis were significantly reduced in BaLKO mouse livers. Hepatic expression of CAR and a panel of genes involved in bile acid modification and transport were also lower in BaLKO mice. Consistently, adenoviral-mediated Baf60a overexpression was sufficient to induce this set of genes in cultured primary hepatocytes and in vivo in the liver. The significance of the alternative pathway was illustrated by significantly reduced bile acid synthesis and pool size in Cyp27a1-null mice (Repa et al., 2000; Rosen et al., 1998). Interestingly, inactivation of Cyp7a1 abolished the primary bile acid biosynthesis pathway and led to induction of the alternative pathway (Ishibashi et al., 1996; Schwarz et al., 1996). Whether Baf60a is required for this compensatory response when the primary bile acid biosynthesis pathway is defective remains unknown. Gain- and loss-of-function studies indicate that Baf60a regulates the expression of the bile acid metabolism gene program in a cell-autonomous manner. At the physiological level, hepatic Baf60a deficiency impaired bile acid production and intestinal cholesterol absorption, resulting in elevated fecal excretion of cholesterol.

Previous studies demonstrated that Baf60a forms a transcriptional complex with PPARα and PGC-1α to regulate fatty acid β-oxidation in hepatocytes (Li et al., 2008). Consistently, mRNA expression of several genes involved in hepatic fat oxidation was reduced in BaLKO mouse livers (data not shown). A somewhat unexpected finding in the current work is that hepatocyte-specific deficiency of Baf60a markedly reduced the expression of CAR. Our gain- and loss-of-function studies demonstrated that Baf60a cell-autonomously induces the expression of CAR through a feedforward regulatory loop. Accordingly, Baf60a deficiency impaired the recruitment of the SWI/SNF complexes, leading to reduced levels of chromatin marks characteristic of

transcriptional activation in hepatocytes. The SWI/SNF ATPase subunit Brm has been shown to interact with Shp and modulate feedback regulation of Cyp7a1 (Kemper et al., 2004). Surprisingly, Baf60a deficiency does not appear to alter Cyp7a1 gene expression. Previous studies demonstrated that TCPOBOP treatments lowered plasma cholesterol levels in mice, in part through increased cholesterol catabolism and inhibition of lipogenesis (Masson et al., 2008; Sberna et al., 2011a, 2011b). It is possible that the discrepancy between these studies and ours is due to whole-body CAR activation versus liver-specific reduction of CAR signaling. Alternatively, it is possible that Baf60a may target other additional transcription factors in the liver to modulate cholesterol metabolism. A future use of the CAR-null mice will help determine the significance of CAR in the regulation of bile acid and cholesterol metabolism by hepatic Baf60a in vivo. Nevertheless, our results strongly suggest that hepatic Baf60a/CAR pathway plays a unique role in bile acid and cholesterol homeostasis. Therapeutic intervention of this pathway in the liver may alter the course of diet-induced hyperlipidemia and reduce the risk of atherosclerosis.

EXPERIMENTAL PROCEDURES

Animal Studies

For the generation of Baf60a liver-specific knockout (BaLKO) mice, a targeting vector that carries two *loxP* sites flanking exons 3 to 5 of mouse Baf60a gene was constructed using BAC recombineering (Figure S1A). C57BL/6J ES cell line (Bruce 4) from Transgenic Animal Model Core at the University of Michigan was chosen for homologous recombination to facilitate breeding into C57BL/6J genetic background for metabolic studies. Transgenic mice expressing the CRE recombinase driven by liver-specific albumin prompter (Alb-CRE) were used to cross with Baf60a flox/flox mice to achieve hepatic-specific deletion of Baf60a. Mice were maintained in 12/12-hr-light/dark cycles and fed with normal rodent chow or Western diet (D12079B, Research Diets) as indicated. All animal studies were performed according to procedures approved by the University Committee on Use and Care of Animals. For in vivo adenovirus transduction, recombinant adenoviruses expressing GFP alone, FH-Baf60a, or FH-CAR were generated using AdEasy adenoviral vector system (Stratagene) and transduced into mice through tail-vein injection. Prior to the final experiments, all adenoviruses were titrated in mice and monitored for the expression of GFP and adenoviral gene AdE4 to ensure similar doses were administered. For ezetimide treatment, ezetimide was suspended in vehicle (0.5% Hydroxyethylcellulose + 0.2% Tween 80) and administered to mice through oral gavage for 4 days. Vehicle alone was used for the control treatment.

Primary Hepatocyte Isolation and Adenovirus Transduction

Primary hepatocytes were isolated using collagenase (type II, Worthington CLS2), as previously described (Li et al., 2008). Cells were maintained in DMEM containing 10% bovine growth serum and transduced with recombinant adenoviruses at similar moiety of infection (MOI) for 24 hr, followed by RNA isolation and gene expression analysis, or ChIP assays.

Coimmunoprecipitation and ChIP

HEK293T cells were transiently transfected with HA-CAR and Myc-Baf60a for 24 hr. Total lysates or immunoprecipitated proteins were analyzed by western blot using antibodies against c-Myc (Sigma, C3956; 1:2,000) or HA (Santa Cruz Biotechnology, sc-66181; 1:2,000). ChIP assay was performed according to the protocol developed by Upstate Biotechnology as described (Meng et al., 2014). In brief, liver nuclei or primary hepatocytes were fixed with 1% formaldehyde and sonicated to produce chromatin lysates. The lysates were pre-cleared with protein G agarose beads and immunoprecipitated overnight with antibodies against Ace-H3 (Millipore, 06-599), H3K4m3 (Millipore,

07-473), Brg1 (Santa Cruz, sc-17796x), or control immunoglobulin G (IgG) in the presence of BSA and salmon sperm DNA. The next day, protein G agarose beads were added to each immunoprecipitation reaction for 1 hr, followed by extensively wash and reverse crosslink. DNA was eluted from the beads and purified using a PCR Purification Kit (Invitrogen) and subsequently analyzed by qPCR using primers located on the proximal CAR promoter. Primers are available upon request.

Gene Expression and Western Blot Analyses

TRIzol reagent (Life Technologies) was used to extract total RNA from tissues and cultured primary hepatocytes. Gene expression analyses were performed using SYBR Green reagent (Life Technologies). Relative abundance of mRNA was normalized to ribosomal protein 36B4. For total protein extracts, frozen liver samples were homogenized in a lysis buffer containing 50 mM Tris (pH 7.5), 150 mM NaCl, 5 mM NaF, 25 mM β-glycerol phosphate, 1 mM sodium orthovanadate, 10% glycerol, 1% Triton X-100, 1 mM DTT, and protease inhibitor cocktail (Roche). For liver nuclear protein extracts, frozen livers were homogenized using a Dounce homogenizer in ice-cold homogenization buffer containing 0.6% NP40, 150 mM NaCl, 10 mM HEPES (pH 7.9), 1 mM EDTA, and protease inhibitor cocktail (Roche). The homogenates were centrifuged at 700 rpm for 1 min at 4°C to remove tissue debris. The suspension was transferred to a new 15-ml tube and centrifuged at 3,000 rpm for 5 min at 4°C. The nuclei pellet was washed with homogenization buffer and resuspended in a low-salt buffer containing 20 mM Tris (pH 7.5), 25% glycerol, 1.5 mM MgCl$_2$, 200 μM EDTA, 20 mM KCl, and protease inhibitor cocktail, followed by the addition of a high-salt buffer (1/2 volume) containing 20 mM Tris (pH 7.5), 1.5 mM MgCl$_2$, 200 μM EDTA, 1.2 M KCl, and protease inhibitor cocktail. The homogenates were rotated for 2 hr at 4°C and centrifuged at 13,000 rpm for 20 min at 4°C to remove the cell debris. For immunoblotting assays, total protein lysates or liver nuclear extracts were separated by SDS-PAGE gels and transferred to a polyvinylidene difluoride membrane (Millipore), followed by immunoblotting with the following primary antibodies. Rabbit polyclonal antibody to Baf60c was generated with the recombinant GST fusion mouse Baf60c protein and affinity purified. Antibody against Baf60a (1:1,000, 611728) was from BD Transduction Laboratories. Antibody against Baf53a (1:1,000, 10341-1-AP) was from Proteintech. Antibody against Lamin A/C (1:2,000, 2032) was from Cell Signaling Technology. Antibodies against c-Myc (1:2,000, C3956) and β-actin (1:2000, A4700) were from Sigma. Antibodies against HA (1:2,000, sc-66181), Brg1 (1:1,000, sc-17796x), Baf155 (1:2,000, sc-10756x), and Baf170 (1:1,000, sc-10757x) were from Santa Cruz. Antibody against LDLR (1:1,000, ab52818) was from Abcam.

Plasma Analysis

For the lipoprotein profiling, pooled plasma samples from three flox/flox or three BaLKO mice were fractionated by fast protein liquid chromatography. The concentrations of cholesterol in each fraction were measured. HDL and VLDL/LDL cholesterol in individual plasma samples were separated and measured using HDL and LDL/VLDL Quantification Colorimetric Kit (BioVision). Plasma concentrations of triglycerides and NEFA were measured using commercial assay kits from Sigma and Wako Diagnostics, respectively. Plasma concentrations of total cholesterol, ALT, and AST were measured using assay kits from Stanbio Laboratory. Plasma Pcsk9 level was measured using the mPcsk9 ELISA kit (Circulex).

^{3}H-Cholesterol Absorption Assay

Acute cholesterol absorption assay was performed as described (Li et al., 2014). Mice were oral gavage with [1,2-^{3}H(N)]-cholesterol (5 mCi and 0.1 mg unlabeled cholesterol in 0.2 ml corn oil). Two hours later, the mice were euthanized, and plasma and liver samples were harvested. Livers were weighed (100 mg/mouse) and homogenized in 1 ml chloroform/methanol (2:1, v/v), followed by rotation at 37°C for 4 hr, and spun at 2,000 × g for 10 min. Radioactivity in triplicate aliquots of plasma and liver extracts was measured by liquid scintillation counting.

Bile Acid Analysis

Control and BaLKO mice fed with WD for 12 weeks were anesthetized. Plasma samples were collected via heart puncture. The gallbladder was removed after common bile duct ligation and transferred to a pre-weighed Eppendorf tube. The bile content in the gallbladder was weighed and converted into volume assuming a density of 1 mg/μl. Liver was dissected, weighed, and homogenized in 75% ethanol. The homogenate was incubated at 50°C for 2 hr to extract bile acids and centrifuged at 6,000 × g for 10 min. Bile acid content in the supernatant was measured. Total bile acid concentrations in plasma, bile, and liver extracts were determined using a Total Bile Acid Assay Kit (BQ 092A-EALD, BQKits).

The concentration of different bile acids in the gallbladder was measured using liquid chromatography-tandem mass spectrometry (LC-MS/MS) as described previously (Perwaiz et al., 2001). In brief, bile samples were diluted 1:200 and 1:10,000 in methanol/water (1:1, v/v). Standard curve was generated with ACS grade analytical standard bile acid compounds in methanol/water (1:1, v/v) via serial dilution using propyl hydroxyl benzoate as internal standard. 10 μl of each sample was loaded to a Thermo Scientific Betabasic-18 100 × 2.1 mm, pore size 5-μm column, eluted with 0.1% formic acid in water as mobile phase A and methanol as mobile phase B in 20 min at 0.2 ml/min, and analyzed with a ABSciex 3200 QTRAP mass spectrometer using negative ESI MRM mode.

The bile acid pool size was measured as previously described (Li et al., 2011). In brief, after the mice were weighed, anesthetized, and exsanguinated, the fresh organs and their contents were collected, minced, and extracted in 20 ml of 95% ethanol at 50°C overnight, followed by spin at 6,000 × g at 4°C for 10 min and collection of the supernatant as extract. The extraction was repeated with another 20 ml of 85% ethanol and 20 ml of 75% ethanol at 50°C for 2 hr, sequentially. All the three extracts were combined and subjected for bile acid measurement using the Bile Acid Assay Kit (BQ 092A-EALD, BQ Kits).

Evaluation of Atherosclerosis

Atherosclerosis studies were conducted as described (Chang et al., 2012). In brief, mice were anesthetized and subjected to whole-body perfusion to fix the tissues. The entire aorta was micro-dissected from each mouse. Atherosclerosis was identified by en face oil red O staining, followed by imaging and lesion area quantification using ImageJ software.

Statistics

Data were analyzed using the unpaired two-tailed Student's t test for independent groups. A p value <0.05 was considered statistically significant.

ACCESSION NUMBERS

The accession number for the microarray data sets reported in this paper is GEO: GSE73709.

SUPPLEMENTAL INFORMATION

Supplemental Information includes three figures and can be found with this article online at http://dx.doi.org/10.1016/j.celrep.2015.10.033.

AUTHOR CONTRIBUTIONS

J.D.L. and Z.-X.M. conceived the project and designed research. Z.-X.M., L.W., L.C., J.S., Y.L., J.B., and Y.E.C. performed the studies. Z.-X.M. and J.D.L. analyzed the data and wrote the manuscript.

ACKNOWLEDGMENTS

REFERENCES

Beaven, S.W., and Tontonoz, P. (2006). Nuclear receptors in lipid metabolism: targeting the heart of dyslipidemia. Annu. Rev. Med. 57, 313–329.

Brown, M.S., and Goldstein, J.L. (1986). A receptor-mediated pathway for cholesterol homeostasis. Science 232, 34–47.

Brown, M.S., and Goldstein, J.L. (2009). Cholesterol feedback: from Schoenheimer's bottle to Scap's MELADL. J. Lipid Res. 50 (Suppl), S15–S27.

Calkin, A.C., and Tontonoz, P. (2012). Transcriptional integration of metabolism by the nuclear sterol-activated receptors LXR and FXR. Nat. Rev. Mol. Cell Biol. 13, 213–224.

Chang, L., Villacorta, L., Li, R., Hamblin, M., Xu, W., Dou, C., Zhang, J., Wu, J., Zeng, R., and Chen, Y.E. (2012). Loss of perivascular adipose tissue on peroxisome proliferator-activated receptor-γ deletion in smooth muscle cells impairs intravascular thermoregulation and enhances atherosclerosis. Circulation 126, 1067–1078.

Chen, W., and Roeder, R.G. (2011). Mediator-dependent nuclear receptor function. Semin. Cell Dev. Biol. 22, 749–758.

Chiang, J.Y. (2009). Bile acids: regulation of synthesis. J. Lipid Res. 50, 1955–1966.

Dasgupta, S., Lonard, D.M., and O'Malley, B.W. (2014). Nuclear receptor co-activators: master regulators of human health and disease. Annu. Rev. Med. 65, 279–292.

Debril, M.B., Gelman, L., Fayard, E., Annicotte, J.S., Rocchi, S., and Auwerx, J. (2004). Transcription factors and nuclear receptors interact with the SWI/SNF complex through the BAF60c subunit. J. Biol. Chem. 279, 16677–16686.

Dong, B., Qatanani, M., and Moore, D.D. (2009). Constitutive androstane receptor mediates the induction of drug metabolism in mouse models of type 1 diabetes. Hepatology 50, 622–629.

Duane, W.C. (1994). Effects of lovastatin and dietary cholesterol on bile acid kinetics and bile lipid composition in healthy male subjects. J. Lipid Res. 35, 501–509.

Evans, R.M., and Mangelsdorf, D.J. (2014). Nuclear Receptors, RXR, and the Big Bang. Cell 157, 255–266.

Expert Panel on Detection, Evaluation, and Treatment of High Blood Cholesterol in Adults (2001). Executive Summary of The Third Report of The National Cholesterol Education Program (NCEP) Expert Panel on Detection, Evaluation, And Treatment of High Blood Cholesterol In Adults (Adult Treatment Panel III). JAMA 285, 2486–2497.

Gao, J., and Xie, W. (2012). Targeting xenobiotic receptors PXR and CAR for metabolic diseases. Trends Pharmacol. Sci. 33, 552–558.

Glass, C.K., and Witztum, J.L. (2001). Atherosclerosis. the road ahead. Cell 104, 503–516.

Goldstein, J.L., and Brown, M.S. (2015). A century of cholesterol and coronaries: from plaques to genes to statins. Cell 161, 161–172.

Goodwin, B., Jones, S.A., Price, R.R., Watson, M.A., McKee, D.D., Moore, L.B., Galardi, C., Wilson, J.G., Lewis, M.C., Roth, M.E., et al. (2000). A regulatory cascade of the nuclear receptors FXR, SHP-1, and LRH-1 represses bile acid biosynthesis. Mol. Cell 6, 517–526.

Grundy, S.M., Cleeman, J.I., Merz, C.N., Brewer, H.B., Jr., Clark, L.T., Hunninghake, D.B., Pasternak, R.C., Smith, S.C., Jr., and Stone, N.J.National Heart, Lung, and Blood Institute; American College of Cardiology Foundation; American Heart Association (2004). Implications of recent clinical trials for the National Cholesterol Education Program Adult Treatment Panel III guidelines. Circulation 110, 227–239.

Horton, J.D., Cohen, J.C., and Hobbs, H.H. (2009). PCSK9: a convertase that coordinates LDL catabolism. J. Lipid Res. 50 (Suppl), S172–S177.

Ishibashi, S., Herz, J., Maeda, N., Goldstein, J.L., and Brown, M.S. (1994). The two-receptor model of lipoprotein clearance: tests of the hypothesis in "knockout" mice lacking the low density lipoprotein receptor, apolipoprotein E, or both proteins. Proc. Natl. Acad. Sci. USA 91, 4431–4435.

Ishibashi, S., Schwarz, M., Frykman, P.K., Herz, J., and Russell, D.W. (1996). Disruption of cholesterol 7alpha-hydroxylase gene in mice. I. Postnatal lethality reversed by bile acid and vitamin supplementation. J. Biol. Chem. 271, 18017–18023.

Kemper, J.K., Kim, H., Miao, J., Bhalla, S., and Bae, Y. (2004). Role of an mSin3A-Swi/Snf chromatin remodeling complex in the feedback repression of bile acid biosynthesis by SHP. Mol. Cell. Biol. 24, 7707–7719.

Lehmann, J.M., Kliewer, S.A., Moore, L.B., Smith-Oliver, T.A., Oliver, B.B., Su, J.L., Sundseth, S.S., Winegar, D.A., Blanchard, D.E., Spencer, T.A., and Willson, T.M. (1997). Activation of the nuclear receptor LXR by oxysterols defines a new hormone response pathway. J. Biol. Chem. 272, 3137–3140.

Li, T., and Chiang, J.Y. (2013). Nuclear receptors in bile acid metabolism. Drug Metab. Rev. 45, 145–155.

Li, S., Liu, C., Li, N., Hao, T., Han, T., Hill, D.E., Vidal, M., and Lin, J.D. (2008). Genome-wide coactivation analysis of PGC-1alpha identifies BAF60a as a regulator of hepatic lipid metabolism. Cell Metab. 8, 105–117.

Li, T., Matozel, M., Boehme, S., Kong, B., Nilsson, L.M., Guo, G., Ellis, E., and Chiang, J.Y. (2011). Overexpression of cholesterol 7α-hydroxylase promotes hepatic bile acid synthesis and secretion and maintains cholesterol homeostasis. Hepatology 53, 996–1006.

Li, P.S., Fu, Z.Y., Zhang, Y.Y., Zhang, J.H., Xu, C.Q., Ma, Y.T., Li, B.L., and Song, B.L. (2014). The clathrin adaptor Numb regulates intestinal cholesterol absorption through dynamic interaction with NPC1L1. Nat. Med. 20, 80–86.

Lu, T.T., Makishima, M., Repa, J.J., Schoonjans, K., Kerr, T.A., Auwerx, J., and Mangelsdorf, D.J. (2000). Molecular basis for feedback regulation of bile acid synthesis by nuclear receptors. Mol. Cell 6, 507–515.

Mahley, R.W. (1988). Apolipoprotein E: cholesterol transport protein with expanding role in cell biology. Science 240, 622–630.

Masson, D., Qatanani, M., Sberna, A.L., Xiao, R., Pais de Barros, J.P., Grober, J., Deckert, V., Athias, A., Gambert, P., Lagrost, L., et al. (2008). Activation of the constitutive androstane receptor decreases HDL in wild-type and human apoA-I transgenic mice. J. Lipid Res. 49, 1682–1691.

Matsubara, T., Li, F., and Gonzalez, F.J. (2013). FXR signaling in the enterohepatic system. Mol. Cell. Endocrinol. 368, 17–29.

Meng, Z.X., Li, S., Wang, L., Ko, H.J., Lee, Y., Jung, D.Y., Okutsu, M., Yan, Z., Kim, J.K., and Lin, J.D. (2013). Baf60c drives glycolytic metabolism in the muscle and improves systemic glucose homeostasis through Deptor-mediated Akt activation. Nat. Med. 19, 640–645.

Meng, Z.X., Wang, L., Xiao, Y., and Lin, J.D. (2014). The Baf60c/Deptor pathway links skeletal muscle inflammation to glucose homeostasis in obesity. Diabetes 63, 1533–1545.

Mottis, A., Mouchiroud, L., and Auwerx, J. (2013). Emerging roles of the core-pressors NCoR1 and SMRT in homeostasis. Genes Dev. 27, 819–835.

Pascussi, J.M., Gerbal-Chaloin, S., Duret, C., Daujat-Chavanieu, M., Vilarem, M.J., and Maurel, P. (2008). The tangle of nuclear receptors that controls xenobiotic metabolism and transport: crosstalk and consequences. Annu. Rev. Pharmacol. Toxicol. 48, 1–32.

Peet, D.J., Turley, S.D., Ma, W., Janowski, B.A., Lobaccaro, J.M., Hammer, R.E., and Mangelsdorf, D.J. (1998). Cholesterol and bile acid metabolism are impaired in mice lacking the nuclear oxysterol receptor LXR alpha. Cell 93, 693–704.

Perwaiz, S., Tuchweber, B., Mignault, D., Gilat, T., and Yousef, I.M. (2001). Determination of bile acids in biological fluids by liquid chromatography-electrospray tandem mass spectrometry. J. Lipid Res. 42, 114–119.

Phelan, M.L., Sif, S., Narlikar, G.J., and Kingston, R.E. (1999). Reconstitution of a core chromatin remodeling complex from SWI/SNF subunits. Mol. Cell 3, 247–253.

Piedrahita, J.A., Zhang, S.H., Hagaman, J.R., Oliver, P.M., and Maeda, N. (1992). Generation of mice carrying a mutant apolipoprotein E gene inactivated

OPEN
ACCESS
CellPress

by gene targeting in embryonic stem cells. Proc. Natl. Acad. Sci. USA *89*, 4471–4475.

Puri, P.L., and Mercola, M. (2012). BAF60 A, B, and Cs of muscle determination and renewal. Genes Dev. *26*, 2673–2683.

Repa, J.J., Lund, E.G., Horton, J.D., Leitersdorf, E., Russell, D.W., Dietschy, J.M., and Turley, S.D. (2000). Disruption of the sterol 27-hydroxylase gene in mice results in hepatomegaly and hypertriglyceridemia. Reversal by cholic acid feeding. J. Biol. Chem. *275*, 39685–39692.

Rosen, H., Reshef, A., Maeda, N., Lippoldt, A., Shpizen, S., Triger, L., Eggertsen, G., Björkhem, I., and Leitersdorf, E. (1998). Markedly reduced bile acid synthesis but maintained levels of cholesterol and vitamin D metabolites in mice with disrupted sterol 27-hydroxylase gene. J. Biol. Chem. *273*, 14805–14812.

Ross, R. (1993). The pathogenesis of atherosclerosis: a perspective for the 1990s. Nature *362*, 801–809.

Saini, S.P., Sonoda, J., Xu, L., Toma, D., Uppal, H., Mu, Y., Ren, S., Moore, D.D., Evans, R.M., and Xie, W. (2004). A novel constitutive androstane receptor-mediated and CYP3A-independent pathway of bile acid detoxification. Mol. Pharmacol. *65*, 292–300.

Sberna, A.L., Assem, M., Gautier, T., Grober, J., Guiu, B., Jeannin, A., Pais de Barros, J.P., Athias, A., Lagrost, L., and Masson, D. (2011a). Constitutive androstane receptor activation stimulates faecal bile acid excretion and reverse cholesterol transport in mice. J. Hepatol. *55*, 154–161.

Sberna, A.L., Assem, M., Xiao, R., Ayers, S., Gautier, T., Guiu, B., Deckert, V., Chevriaux, A., Grober, J., Le Guern, N., et al. (2011b). Constitutive androstane receptor activation decreases plasma apolipoprotein B-containing lipoproteins and atherosclerosis in low-density lipoprotein receptor-deficient mice. Arterioscler. Thromb. Vasc. Biol. *31*, 2232–2239.

Schwarz, M., Lund, E.G., Setchell, K.D., Kayden, H.J., Zerwekh, J.E., Björkhem, I., Herz, J., and Russell, D.W. (1996). Disruption of cholesterol 7alpha-hydroxylase gene in mice. II. Bile acid deficiency is overcome by induction of oxysterol 7alpha-hydroxylase. J. Biol. Chem. *271*, 18024–18031.

Schwarz, M., Russell, D.W., Dietschy, J.M., and Turley, S.D. (2001). Alternate pathways of bile acid synthesis in the cholesterol 7alpha-hydroxylase knockout mouse are not upregulated by either cholesterol or cholestyramine feeding. J. Lipid Res. *42*, 1594–1603.

Steinberg, D. (2002). Atherogenesis in perspective: hypercholesterolemia and inflammation as partners in crime. Nat. Med. *8*, 1211–1217.

Sudarsanam, P., and Winston, F. (2000). The Swi/Snf family nucleosome-remodeling complexes and transcriptional control. Trends Genet. *16*, 345–351.

Thomas, C., Pellicciari, R., Pruzanski, M., Auwerx, J., and Schoonjans, K. (2008). Targeting bile-acid signalling for metabolic diseases. Nat. Rev. Drug Discov. *7*, 678–693.

Tiemann, M., Han, Z., Soccio, R., Bollineni, J., Shefer, S., Sehayek, E., and Breslow, J.L. (2004). Cholesterol feeding of mice expressing cholesterol 7alpha-hydroxylase increases bile acid pool size despite decreased enzyme activity. Proc. Natl. Acad. Sci. USA *101*, 1846–1851.

Wang, W., Xue, Y., Zhou, S., Kuo, A., Cairns, B.R., and Crabtree, G.R. (1996). Diversity and specialization of mammalian SWI/SNF complexes. Genes Dev. *10*, 2117–2130.

Waters, D.D., Brotons, C., Chiang, C.W., Ferrières, J., Foody, J., Jukema, J.W., Santos, R.D., Verdejo, J., Messig, M., McPherson, R., et al.; Lipid Treatment Assessment Project 2 Investigators (2009). Lipid treatment assessment project 2: a multinational survey to evaluate the proportion of patients achieving low-density lipoprotein cholesterol goals. Circulation *120*, 28–34.

Wilson, B.G., and Roberts, C.W. (2011). SWI/SNF nucleosome remodellers and cancer. Nat. Rev. Cancer *11*, 481–492.

Wu, J.I., Lessard, J., and Crabtree, G.R. (2009). Understanding the words of chromatin regulation. Cell *136*, 200–206.

Xu, G., Salen, G., Shefer, S., Tint, G.S., Nguyen, L.B., Chen, T.S., and Greenblatt, D. (1999). Increasing dietary cholesterol induces different regulation of classic and alternative bile acid synthesis. J. Clin. Invest. *103*, 89–95.